

INITIAL ERROR ANALYSIS FOR THE LHC COLLIMATION INSERTIONS

D.I.Kaltchev, M.K.Craddock¹, R.V. Servranckx,
 TRIUMF, 4004 Wesbrook Mall, Vancouver, B.C., Canada V6T2A3
 J.B.Jeanneret, CERN, CH-1211 Geneva 23, Switzerland

Abstract

The two cleaning insertions in the LHC, for betatron and momentum collimation, are optimized for an ideal lattice and collimator jaw setup. We have studied a collimation beam line with randomly generated jaw misalignments and quadrupole field and alignment errors, the resultant distortion of the reference orbit being corrected with the help of monitors placed near critical collimators. Different closed orbit errors and beam shapes are considered at the entrance. We report the level of errors for which no corrections are needed and the level for which corrections are not possible.

1 INTRODUCTION

The optics of the LHC betatron and momentum collimation insertions, and the locations and orientations of the collimator jaws, have been optimized so that the secondary halos, produced by scattering of circulating protons at the primary collimators, are restricted to the desired aperture [1]. The halo is defined as the beam of scattered particles within solid angle 2π – with initial non-normalized coordinates (x, y) (a point-like source on the primary collimator jaw surfaces) and initial angles (x', y') within $(-\frac{\pi}{2}, \frac{\pi}{2})$.

We have studied how the collimation quality is affected by jaw and quadrupole alignment errors, quadrupole powering errors, and incoming beam positioning and mismatch. Since each warm quadrupole Q6L-Q6R consists of a group of 5-6 modules, both group and module misalignment has been considered. As a reference case without errors, we use the optimized layout for the betatron insertion IR7 (Fig. 1), with the primary collimator apertures set to 6σ , and 16 secondaries set to 7σ (injection optics). For this the halo particles escaping all secondary jaws are found to have a maximum combined transverse invariant $A = \sqrt{X^2 + X'^2 + Y^2 + Y'^2}$ of 8.4 in units of σ , while the maximum in-plane invariants are $A_x = 7.83, A_y = 8.16$.

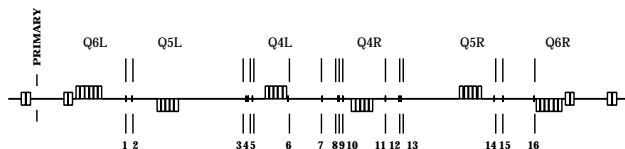


Figure 1: Betatron cleaning insertion layout.

¹ Also at Dept. of Physics & Astronomy, UBC, Vancouver, Canada.

2 ERROR ANALYSIS

The effects of quadrupole misalignments and powering errors were studied by using the code DIMAD [2] to trace the following beam parameters through IR7: reference orbit $x_{orb}, x'_{orb}, y_{orb}, y'_{orb}$, beta functions β_x, β_y and betatron phases μ_x, μ_y . Their values, computed at the secondary jaws, are passed to the code Distribution of Jaws (DJ) which finds the maximum invariants A, A_x and A_y of surviving halo particles. Orbit positioning errors and beam mismatch at the primary are taken into account by using nonzero initial values $x_{orb}^{(in)}, x'_{orb}^{(in)}, y_{orb}^{(in)}, y'_{orb}^{(in)}$ and initial beta functions $\beta_x^{(in)}, \beta_y^{(in)}$ different from the nominal ones.

In DJ, for a fixed set of halo sources, the jaw phases $\mu_x^{(k)}, \mu_y^{(k)}$ ($k=1, \dots, 16$) define A, A_x and A_y in the following way [1]: all jaws (pairs of parallel lines in normalized $X-Y$ space) are transformed (rotated by angles $\mu_x^{(k)}, \mu_y^{(k)}$) to the entrance, and the “escape window” in initial-angle space is found – its vertices giving A, A_x and A_y . This procedure is equivalent [1] to linear tracking with the maximum escape angles being recorded, but is much faster.

To include the *misalignment of a pair of jaws* in this model, the corresponding pair of lines is displaced from the origin in normalized $X-Y$ space by $\Delta x_{jaw_k} / \sqrt{\beta_{x,k}}$ and $\Delta y_{jaw_k} / \sqrt{\beta_{y,k}}$, in effect changing the escape window. Here $\Delta x_{jaw_k}, \Delta y_{jaw_k}$ are the horizontal and vertical displacements of the midpoint (centre) of the pair with respect to the reference orbit, which passes through the quadrupole centers. If the reference orbit at the k -th jaw is displaced by $x_{orb}^{(k)}$ with respect to the vacuum chamber axis, the jaw displacement in DJ is taken to be $\Delta x_{jaw_k} = -x_{orb}^{(k)}$ (and similarly for y).

Powering errors and incoming beam mismatch lead to different sets of jaw phases relative to the error-free case.

Orbit correction was performed by DIMAD, with 6 correctors and 6 double (horizontal and vertical) beam position monitors placed in the middle of each of the quadrupole groups (Fig 1), plus one additional vertical corrector at the beam line entrance. The orbit displacements at the monitors are minimized by the least square method.

Monitor alignment errors with respect to the vacuum chamber axis (rms lateral displacements $\sigma_{x,mon}, \sigma_{y,mon}$) are simulated by random misalignment of the jaws with respect to the reference orbit with the same rms values.

For all errors together, the tolerable increase in A is assumed to be $\approx \sigma$, i.e. the maximum acceptable value is 9.5.

Table 2: Effects of random lateral misalignment of all quadrupoles, with and without orbit correction.

$\sigma_x = \sigma_y$ [μm]		100	200	400
As modules				
No corr.	$max_{10} \hat{x}_{orb}/\hat{y}_{orb}$ [mm]	0.5 / 0.7	1.0 / 1.4	2.1 / 2.9
	$max_{10} \hat{x}_{orb}^{jaw}/\hat{y}_{orb}^{jaw}$ [mm]	0.5 / 0.6	1.0 / 1.3	1.9 / 2.5
	$max_{10} A/A_x/A_y$	8.7 / 8.1 / 8.3	9.1 / 8.7 / 8.5	10.2 / 9.8 / 8.9
	$ave_{10} A/A_x/A_y$	8.5 / 7.8 / 8.1	8.7 / 8 / 8	9.1 / 8.3 / 8.0
As groups				
No corr.	$max_{10} \hat{x}_{orb}/\hat{y}_{orb}$ [mm]	1.8 / 1.1	3.6 / 2.2	7.2 / 4.5
	$max_{10} \hat{x}_{orb}^{jaw}/\hat{y}_{orb}^{jaw}$ [mm]	1.5 / 1	2.9 / 2.1	5.8 / 4.1
	$max_{10} A/A_x/A_y$	9.9 / 9.3 / 9.2	11.6 / 10.8 / 10.3	14.5 / 14 / 11.6
	$ave_{10} A/A_x/A_y$	9.1 / 8.4 / 8.4	9.9 / 9.0 / 8.6	11.5 / 10.4 / 9.2
	$max_{10} x_{orb}^{end}/x_{orb}'^{end}/y_{orb}^{end}/y_{orb}'^{end}$ [mm] / μrad	0.8 / 10 / 0.6 / 14	1.5 / 20 / 1.2 / 28	3 / 41 / 2.4 / 56
	$ave_{10} x_{orb}^{end}/x_{orb}'^{end}/y_{orb}^{end}/y_{orb}'^{end}$ [mm] / μrad	0 / 1 / 0.2 / 4	0.1 / 3 / 0.3 / 7	0.2 / -5 / 0.6 / -15
With orbit corr.	$max_{10} \hat{x}_{orb}, \hat{y}_{orb}$ [mm]	0.2 / 0.2	0.3 / 0.3	0.7 / 0.7
	$max_{10} \hat{x}_{orb}^{jaw}, \hat{y}_{orb}^{jaw}$	0.1 / 0.2	0.2 / 0.3	0.4 / 0.6
	$max_{10} A/A_x/A_y$	8.6 / 8.0 / 8.2	8.7 / 8.2 / 8.3	9.1 / 8.6 / 8.5
	$ave_{10} A/A_x/A_y$	8.5 / 7.8 / 8.1	8.5 / 7.9 / 8.1	8.7 / 7.9 / 8.1
	$max_{10} x_{orb}^{end}/x_{orb}'^{end}/y_{orb}^{end}/y_{orb}'^{end}$ [mm]/[μrad]	0 / 1 / 0 / 2	0 / 3 / 0 / 4	0.1 / 6 / 0 / 8
	max. corr. [μrad]	6	12	24
Jaws 9,16	$max_{10} A/A_x/A_y$	8.5 / 8.0 / 8.2	8.6 / 8.1 / 8.3	8.9 / 8.4 / 8.4

3 ERROR ANALYSIS RESULTS

Analysis of *individual jaw misalignment* for horizontal displacements (Fig. 2) shows that A is most sensitive to lateral shifts of jaws 8, 9 and 16. Similar behavior was observed in the vertical plane.

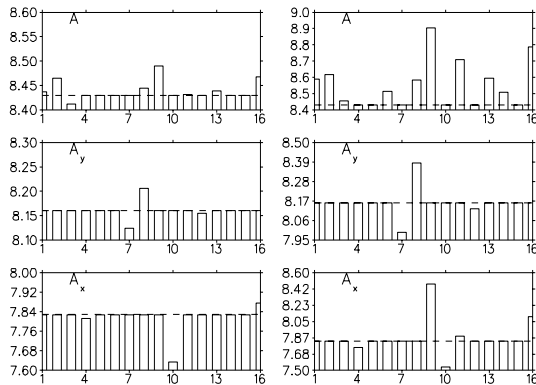


Figure 2. Effect of horizontal displacement of individual jaws: left: 0.1 mm; right: 0.5 mm.

Table 1 shows the effects of individual quadrupole group misalignment and group powering errors on A (nominal value 8.4). Left: horizontal/vertical displacement 100 and 200 μm . Right: relative field error 5×10^{-3} . Transverse shifts of 0.1 – 0.2 mm lead to 0.5 – 1σ loss in collimation quality. Quadrupole powering errors up to the level 10^{-3} have little effect on A (see also **Table 3**).

Table 2 presents results from *random transverse misalignment of quadrupoles*. For each seed, Q6L-Q6R were

Table 1

	Displacement hor. / vert. [μm]		Rel. field error $\Delta k_1 / k_1$
	100	200	5×10^{-3}
Q6L	8.8 / 8.7	8.6 / 9.4	8.5
Q5L	8.5 / 8.6	8.5 / 8.7	8.5
Q4L	8.7 / 8.6	8.5 / 9.1	8.5
Q4R	8.5 / 8.7	8.5 / 8.5	8.4
Q5R	8.5 / 8.3	8.3 / 8.6	8.4

randomly displaced with Gaussian distributions in both x and y planes, with equal rms values 0.1, 0.2 and 0.4 mm, truncated at 2σ . Here $\hat{x}_{orb} = \max |x_{orb}|$ is the maximum absolute value of horizontal orbit excursion along the beam line and $\hat{x}_{orb}^{jaw} = \max_k |x_{orb}^{(k)}|$ is the maximum excursion at a jaw (similarly for y). Also max_{10} and ave_{10} denote the maximum and the average values of 10 seeds, and superscript *end* is used for the residual orbit displacement and angle at the beam line exit. For example, for an rms displacement of 0.2 mm of all groups, the “worst” of the 10 seeds produces $A=11.6$ with residual horizontal orbit displacement at the exit $x_{orb}^{end} = 1.5$ mm, and $x_{orb}'^{end} = 0.02$ mrad. The 10-seed averaged values are $A=9.9$, $x_{orb}^{end} = 0.1$ mm and $x_{orb}'^{end} = 0.003$ mrad.

In so far as the alignment of individual modules within a group is expected to be better than alignment of the groups with respect to each other, an appropriate orbit correction is absolutely necessary, since group alignment errors of 100 – 200 μm will very likely be present. The same seed sequence was used both with and without correction. The last row

of Table 2 shows the effect of two monitors being relocated from the closest quadrupoles to the critical locations near jaws 9 and 16 identified in Fig. 2.

Table 3: Random powering errors in all quadrupoles.

$\Delta K_1 / K_1$	10^{-3}	5×10^{-3}
$max_{10} A/A_x/A_y$	8.4/7.9/8.2	8.6/7.9/8.3
$ave_{10} A/A_x/A_y$	8.4/7.8/8.15	8.5/7.8/8.2

Table 4: Incoming beam steering.

Horizontal [mm,mrad]			
$(x_{orb}^{(in)}, x'_{orb}{}^{(in)})$		(1, 0)	(0, 0.02)
No corr.	\hat{x}_{orb}	3.5	2.4
	\hat{x}_{orb}^{jaw}	3.2	1.9
	$A/A_x/A_y$	11.1/10.5/8.7	9.5/8.5/8.2
	$x_{orb}^{end}/x'_{orb}{}^{end}$	1.5/7	0.5/16
With corr.	\hat{x}_{orb}	1	1.2
	\hat{x}_{orb}^{jaw}	0.6	0.9
	$A/A_x/A_y$	8.7/7.9/8.2	8.8/7.9/8.1
	$x_{orb}^{end}/x'_{orb}{}^{end}$	0/0	0/0
max. corr.			
2.2			
4.4			
Vertical [mm,mrad]			
$(y_{orb}^{(in)}, y'_{orb}{}^{(in)})$ [mm,mrad]		(1, 0)	(0, 0.02)
No corr.	\hat{y}_{orb}	2.8	4.7
	\hat{y}_{orb}^{jaw}	2.4	3.4
	$A/A_x/A_y$	10.7/8.6/10.6	10.8/7.9/10.4
	$y_{orb}^{end}/y'_{orb}{}^{end}$	0.7/7	0.4/33
With corr.	\hat{y}_{orb}	1	1.1
	\hat{y}_{orb}^{jaw}	0.4	0.4
	$A/A_x/A_y$	8.5/7.8/8.2	8.6/7.8/8.2
	$y_{orb}^{end}/y'_{orb}{}^{end}$	0/0	0/0
max. corr.			
2.2			
53			

 Table 5: $\Delta\beta^{(in)}/\beta^{(in)} = 10\%$

	Hor.	Vert.
$A/A_x/A_y$	8.6/8/8.2	8.8/7.7/8.4

Tables 4 and 5 show the effect of a fixed incoming beam steering error in position (+1 mm) or angle (+0.02 mrad), either horizontal or vertical, and of 10% incoming beam mismatch.

Table 6 shows the effect of random misalignment of all jaws with rms values 0.2 and 0.4 mm. This is equivalent to introducing monitor misalignment (orbit measurement) errors of the same magnitude.

Table 7 was obtained with all errors together, at the acceptable level for each, as follows:

Fixed incoming beam steering error:

$$(x_{orb}^{(in)}, x'_{orb}{}^{(in)}, y_{orb}^{(in)}, y'_{orb}{}^{(in)}) = (0.5, 0, 0.5, 0) [\text{mm/mrad}];$$

$$\text{Beam mismatch: } \Delta\beta_x^{(in)}/\beta_x^{(in)} = \Delta\beta_y^{(in)}/\beta_y^{(in)} = 0.1;$$

Quadrupole misalignment: $\sigma_x = \sigma_y = 250 \mu\text{m}$;

Quadrupole powering errors: $\Delta k_1/k_1 = 1 \times 10^{-3}$;

Monitor misalignment: $\sigma_{x,mon} = \sigma_{y,mon} = 250 \mu\text{m}$;

Orbit correction: as outlined above.

The largest A -values ($A > 9.5$) in Table 7 correspond to a few seeds (1-3 out of 40 for several different seed

 Table 6: Monitor alignment [μm]

$\sigma_{x,mon} = \sigma_{y,mon}$	200	400
$max_{10} A/A_x/A_y$	8.8/8.4/8.2	9.3/8.2/9.1
$ave_{10} A/A_x/A_y$	8.7/7.8/8.1	9.0/7.8/8.3

Table 7: All errors together.

All jaws $\sigma_{x,mon} = \sigma_{y,mon} = 0.25 \text{ mm}$	
$max_{40} \hat{x}_{orb}/\hat{y}_{orb}$ [mm]	1/0.9
$max_{40} \hat{x}_{orb}^{jaw}/\hat{y}_{orb}^{jaw}$	0.4/0.4
$max_{40} A/A_x/A_y$	10.1/9/9
$ave_{40} A/A_x/A_y$	9.2/8.1/8.4
$max_{40} x_{orb}^{end}/x'_{orb}{}^{end}/y_{orb}^{end}/y'_{orb}{}^{end}$ [mm] / [μrad]	0.1/5/0/6
max. corrector [μrad]	26
$\sigma_{x,mon} = \sigma_{y,mon} = 0.1 \text{ mm}$ at jaws 8, 9	
$max_{40} A/A_x/A_y$	9.5/8.8/8.9
$ave_{40} A/A_x/A_y$	9.2/8./8.4

sequences), for which the random orbit and jaw displacements add up at some jaws. Most critical appear to be jaws 8 and 9 (spaced $\sim 3 \text{ m}$ apart) located in a region with a low horizontal beta function. Setting the monitor error at these jaws to $100 \mu\text{m}$ decreases the difference between maximum and average A -values from σ to 0.5σ . Table 8 demonstrates this for three beam steering errors.

Table 8.

steering error	rms monitor error 0.25 mm		rms monitor error=0.1 mm at jaws 8 and 9	
	$max_{40} A$	$ave_{40} A$	$max_{40} A$	$ave_{40} A$
0.5	10.1	9.2	9.5	9.2
0.3	10.1	9.2	9.4	9.1
0.1	9.9	9.1	9.4	9.1

4 CONCLUSIONS

We have found that the following combined misalignments and errors lead to less than 1σ increase in the maximum amplitude A of escaping particles:

- 1) fixed incoming beam steering errors below 0.5 mm in both transverse planes (with zero initial angles);
- 2) monitors and quadrupoles randomly displaced $250 \mu\text{m}$ rms in each transverse direction with respect to the central axis of the primary jaws (with the exception of jaws 8 and 9, where the maximum monitor error used was $100 \mu\text{m}$);
- 3) incoming beam mismatch below 10%;
- 4) quadrupole powering errors below 10^{-3} .

Under these conditions the local correction has only a small effect on the rest of the ring – the exit orbit displacement is zero and the exit angle $< 0.01 \text{ mrad}$.

5 REFERENCES

- [1] D. Kaltchev, M. K. Craddock, R.V. Servranckx and J.B. Jeanneret, *Proc. PAC97, Vancouver*, ed. M. Comyn et al. (IEEE, 1998) p. 153; CERN LHC Project Report 134 (1997).
- [2] R.V.Servranckx, *User's Guide to the Program Dimad*, TRIUMF Design Note, TRI-DN-93-K233, (1993).